Thermal Protection System Aerothermal Screening Tests in the HYMETS Facility

Christine E. Szalai[1]
Jet Propulsion Laboratory, California Institute of Technology, Pasadena, CA, 91109

Robin A.S. Beck[2] and Matthew J. Gasch[3]
NASA Ames Research Center, Moffett Field, CA, 94035

Antonella I. Alunni[4] and Jose F. Chavez-Garcia[5]
ERC, Inc., Moffett Field, CA, 94035

Scott C. Splinter[6] and Jeffrey G. Gragg[7]
NASA Langley Research Center, Hampton, VA, 23681

and

Amy Brewer[8]
Analytical Services and Materials, Inc., Hampton, VA, 23666

The Entry, Descent, and Landing (EDL) Technology Development Project has been tasked to develop Thermal Protection System (TPS) materials for insertion into future Mars Entry Systems. A screening arc jet test of seven rigid ablative TPS material candidates was performed in the Hypersonic Materials Environmental Test System (HYMETS) facility at NASA Langley Research Center, in both an air and carbon dioxide test environment. Recession, mass loss, surface temperature, and backface thermal response were measured for each test specimen. All material candidates survived the Mars aerocapture relevant heating condition, and some materials showed a clear increase in recession rate in the carbon dioxide test environment. These test results supported subsequent down-selection of the most promising material candidates for further development.

I. Introduction

IN support of the Entry, Descent, and Landing (EDL) Technology Development Project (TDP), a screening arc jet test of rigid ablative thermal protection systems (TPS) was performed in the Hypersonic Materials Environmental Test System (HYMETS) facility at NASA Langley Research Center.

The primary goal of the TPS development element of the TDP is to develop rigid and flexible TPS materials capable of withstanding the severe aerothermal loads associated with aerocapture and entry into the Martian atmosphere, while significantly reducing the TPS mass fraction contribution to the entry system. Significant advancements in TPS materials technology are needed in order to enable the successful delivery of heavy mass payloads to the Martian surface for robotic precursor and subsequent human exploration missions. The goal of the TPS development element is to advance low Technology Readiness Level (TRL) rigid ablative material concepts to

---

[1] Senior Systems Engineer, EDL Systems and Advanced Technologies, 4800 Oak Grove Dr., M/S 301-490, non-member.
[2] Aerospace Engineer, Entry Systems and Vehicle Development Branch, M/S 229-1, Associate Fellow.
[3] Research Scientist, Thermal Protection Materials Branch, M/S 234-1, Member.
[4] Research Scientist, Thermal Protection Materials Branch, M/S 234-1, non-member.
[5] Aerospace Engineer, Thermophysics Facilities Branch, M/S 229-1, non-member.
[6] Aerospace Engineer, Structural Mechanics and Concepts Branch, M/S 190, Member.
[7] Engineering Technician, Structures Experiments Branch, M/S 188D, non-member.
[8] Senior Test Engineer, Analytical Services and Materials, Inc., M/S 190, non-member.

TRL 5 by FY14, and promising flexible material concepts to TRL 4 by FY14. This test series evaluated rigid ablative material concepts only.

In the early phases of the TPS development task, the goal is to identify as many promising material candidates as possible, and then perform cost efficient screening tests to obtain preliminary ablative, thermal, and structural performance data in order to assess the potential of the material concept to meet key performance parameters defined by the TPS project element.[1] The evaluation of screening test data supports subsequent down-selection of the most promising material candidates.

Four vendors were selected to provide rigid ablative test specimens for Phase 1 screening tests: 1) Applied Research Associates (ARA), providing Poly-Imide Refractory Ablator System (PIRAS-22) and PhenCarb test specimens, 2) Boeing, providing Boeing Phenolic Ablator (BPA) test specimens, 3) Lockheed Martin Space Systems, providing Carbon-Carbon/CalCarb and MonA (Monolithic Ablator) test specimens, and 4) Textron, providing 3-Dimensional Quartz Phenolic (3DQP) and Avcoat test specimens. Phenolic Impregnated Carbon Ablator (PICA), considered the current state-of-the-art and manufactured by Fiber Materials, Inc. (FMI), was also included in this test series.

This Phase I screening test series had the following test objectives:

1) Assess survivability of material concepts at relevant Mars aerocapture heating conditions in both air and Martian plasma environments
2) Obtain recession data for material concepts at relevant Mars aerocapture heating conditions in both air and Martian plasma environments
3) Obtain surface temperature and backface thermal response of material concepts at relevant Mars aerocapture heating conditions in both air and Martian plasma environments

The HYMETS facility has the capability of simulating heating conditions similar to those expected in a Martian atmospheric entry. Of note, HYMETS has the capability to test in a simulated Martian atmosphere of primarily carbon dioxide.

II. Test Facility

The HYMETS facility, shown in Figure 1, is configured with a segmented constrictor dc-electric arc heater as an arc plasma generator. Test gasses are injected tangentially into the bore of the arc plasma generator at seven discrete locations, and are heated by a high-voltage arc column maintained between the electrodes to create the high temperature ionized arc plasma flow. Several compressed gas cylinders supply the test gasses used in the arc plasma generator, and can be custom mixed to any desired test atmosphere. Currently established test atmospheres in HYMETS are for a simulated Standard Earth atmosphere (5% Ar, 75% N_2, and 20% O_2 for a 79% N_2 to 21% O_2 ratio) and a simulated Martian atmosphere (71% CO_2, 24% N_2, and 5% Ar for a 75% CO_2 to 25% N_2 ratio). To prevent excessive electrode oxidation in its current configuration, the simulated Martian atmosphere is not quite that of the actual Martian atmosphere (i.e. 95% CO_2, 3% N_2, and 1.6% Ar). Nitrogen and Argon are used as shield gasses near the cathode and anode, respectively, to protect the electrodes from rapid oxidation.[2]

The test sample and instrumentation probes are mounted on four water-cooled injection stings arranged symmetrically around the inside circumference of the test chamber at a distance of approximately 2.5 inches from the nozzle exit, and are inserted into the arc plasma flow by the touch screen operations module. Figure 2 shows a sample inside the HYMETS test chamber.

For this test series, the instrumentation used in the HYMETS facility consisted of a pitot tube, which measured stagnation pressure, and a copper slug calorimeter, which measured cold wall heat flux. The pitot tube and slug calorimeter were inserted into the flow prior to the test article for each test run.

A two-color (ratio) pyrometer and full color digital video camera with variable exposure settings were positioned outside the test chamber and remotely aimed through a viewport on the test chamber door by the HYMETS technician during testing. The bulk enthalpy of the plasma flow was determined using a thermopile to measure the differential temperature across the inlet and outlet of the cooling water manifolds for the arc plasma generator, and flow meters to measure the mass flow rates for both the cooling water and the arc plasma generator test gas.

In order to evaluate whether the performance of the materials is consistent with what is expected, a comprehensive knowledge of the arc jet stream conditions is required. This is accomplished through flow characterization and Computational Fluid Dynamics (CFD) analysis. Flow characterization efforts for the HYMETS facility have recently been initiated, but are not yet complete. Since the objective of this test series was material screening at the same test conditions, material performance comparisons were made in a relative sense, without supporting material response analytical predictions.

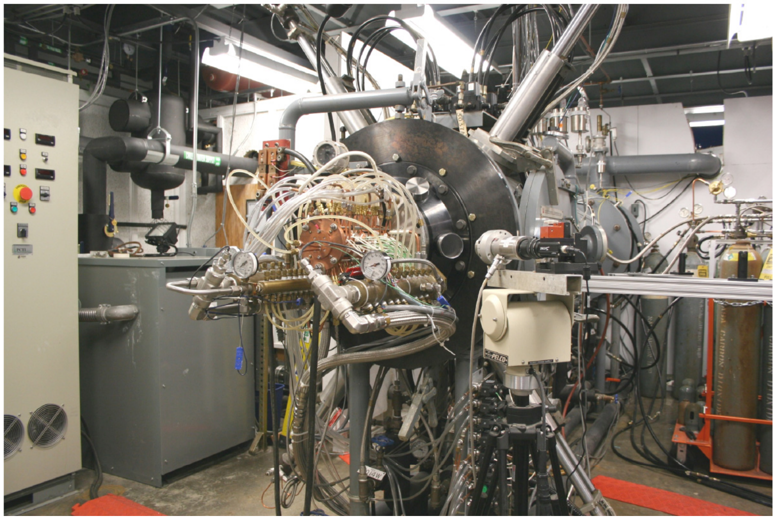

Figure 1. Exterior of the HYMETS facility

Figure 2. Instrumentation probe arrangement and test sample positioned inside HYMETS test chamber

III. Test Condition

The test condition for this test series is provided in Table 1. This test requirement is derived from aerothermal analyses of a mid Lift/Drag (L/D) ellipsled concept from the EDL-Systems Analysis Mars Design Reference Architecture 5.0. A dual-pulse aerothermal environment resulted from aerocapture and entry trajectory designs, with the peak heating rate predicted to occur during the aerocapture maneuver (Figure 3).[1] In addition, the peak stagnation pressure predicted for the aerocapture is 45 kPa. While testing at the peak heating rate of 500 W/cm^2 and the peak stagnation pressure of 45 kPa is desired, current facility capabilities limit the maximum heating on the 1.3-inch diameter samples to 300 W/cm^2 at a stagnation pressure of 3.5 kPa. Since this was a screening test, all test specimens were tested at the same heating and pressure condition, in both air and Mars simulated atmospheric test environments.

Table 1. Test Condition

Material	Facility	Sample Size	Heat Flux	Stagnation Pressure	Bulk Enthalpy	Duration
Rigid Ablative TPS materials	HYMETS (LaRC)	1.3-inch outer diameter	300 W/cm^2	3.5 kPa	33.5 kJ/g	15 seconds (nominal)

Due to initial uncertainty about material performance in the HYMETS facility, a nominal test duration was established through tests prior to the start of the screening test series. PICA has the lowest density of the material sample set and was thus expected to have the highest recession. PICA samples were tested at various test durations to assess the resulting amount of recession and char depth. Figure 4 shows cross section views of PICA samples tested at durations from 5 to 20 seconds, at the heating rate and stagnation pressure specified in Table 1. A test duration of 20 seconds shows that the sample charred through the entire sample thickness, which is not desirable for material performance evaluation. A test duration of 15 seconds resulted in meaningful recession with a char depth less than the sample thickness. Ideally, test times should be identical for each material type, but due to varying densities and material types, test durations varied across the test matrix in order to achieve meaningful recession without overheating the backface.

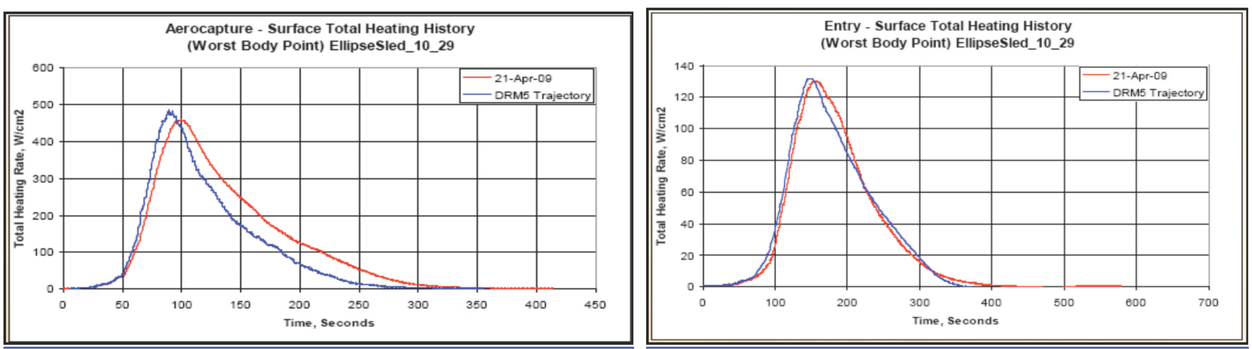

Figure 3. Aerocapture and entry heating rates for the mid lift/drag aeroshell

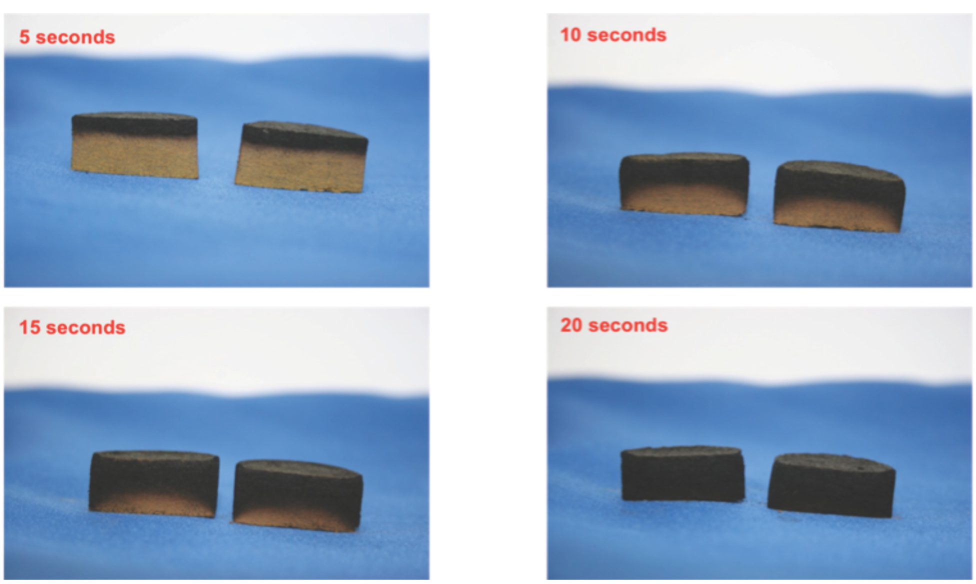

Figure 4: Cross section views of PICA samples tested to establish nominal test condition

IV. Rigid Ablative Material Test Samples

Four vendors were selected to provide seven different types of rigid ablative materials for this screening test. In addition, Phenolic Impregnated Carbon Ablator (PICA) test articles were included in this test series since PICA is considered the current state-of-the-art. Nominally, two test articles would be tested in air and two articles would be tested in a simulated Martian atmospheric environment. The fifth sample would be available as a spare in case of any problems encountered in the nominal test matrix. A summary of the material types, vendors, and average bulk density of the five specimens is shown in Table 2.

ARA's Ablatives Laboratory provided Poly-Imide Refractory Ablator System (PIRAS-22) and PhenCarb-28 test specimens. PIRAS-22 is a polyimide thermoplastic ablator system containing reinforcing fibers and fillers. PhenCarb-28 is a phenolic thermoplastic ablator system that contains a cured phenolic polymer resin combined with reinforcing fibers, low-density fillers, and honeycomb reinforcement.

Boeing provided test specimens of the outer ablative layer of the Boeing Phenolic Ablator-Functionally Graded (BPA-FG) material system. The BPA-Low Cure Temperature outer layer is a medium-density phenolic syntactic foam.

Lockheed Martin Space Systems provided the outer carbon-carbon layer of the Carbon-Carbon/CalCarb (CC/CalCarb) material system and Monolithic Ablator (MonA) test specimens. The CC/CalCarb dual layer material system is an improvement over the Genesis heatshield, consisting of an advanced carbon-carbon facesheet over carbon foam insulation. While these carbon-carbon test articles had the highest density of all test specimens (1.56 g/cc), as a dual layer system with the low-density carbon insulative layer, CC/CalCarb has a typical bulk density of only 0.24 g/cc. The MonA material consists of a PICA-like mixture packed into a honeycomb reinforcement, which is then cured.

Textron provided Avcoat and 3-Dimensional Quartz Phenolic (3DQP) test specimens. Avcoat was originally developed in the 1960s for the Apollo Command Module heatshield, and production has recently been restarted in support of the Crew Exploration Vehicle heatshield. It is a glass-filled epoxy-novolac system with honeycomb structural reinforcement. The 3DQP dual layer specimens consist of a high-density quartz-phenolic outer layer over an insulative inner layer.

Residual PICA material from the manufacture of the Mars Science Laboratory heatshield was utilized to produce the PICA test specimens. This PICA material was manufactured by Fiber Materials, Inc. The material consists of a low density, fibrous carbon substrate infiltrated with phenolic resin. These PICA test articles had the lowest density of all materials tested at an average bulk density of 0.273 g/cc.

Table 2. Rigid Ablative Material Summary

Material	Vendor	Average Bulk Density of Test Specimens (g/cc)
PIRAS-22	Applied Research Associates	0.367
PhenCarb	Applied Research Associates	0.467
BPA	Boeing	0.450
Carbon-Carbon	Lockheed Martin	1.560
MonA	Lockheed Martin	0.318
Avcoat	Textron	0.536
3DQP	Textron	1.012
PICA	Fiber Materials, Inc.	0.273

Ablator test specimens consisted of 1-inch-diameter pucks with a thickness of 0.5 inches as shown in Figure 5, and included one Type K backface thermocouple. A thin Reusable Surface Insulation (RSI) spacer was bonded to the back of the test specimen to provide insulation from the copper model holder and to encapsulate the backface thermocouple. The test specimen assembly is shown in Figure 6 and consisted of a silicon carbide coated graphite cap, the test specimen, a spacer, and the water-cooled copper mount, which was affixed to the injection sting. The test specimen and the spacer were gently compressed between the graphite cap and the copper mounting, and were threaded into place on the injection sting. The outer diameter of the assembly was 1.3 inches.

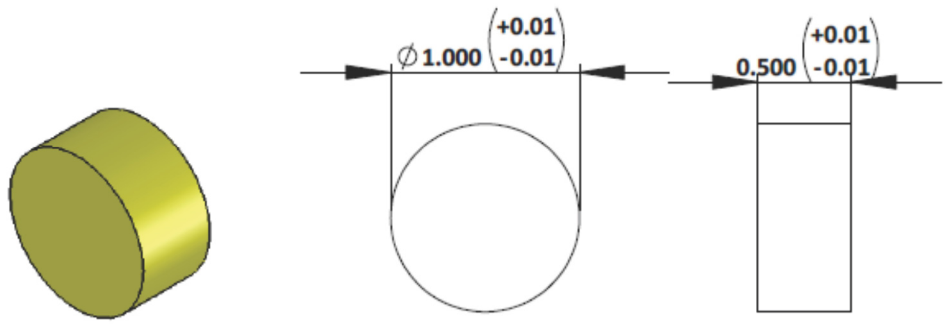

Figure 5. Rigid ablator test specimen dimensions (inches)

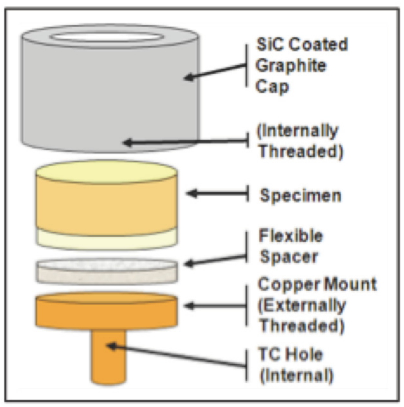

Figure 6. HYMETS test specimen assembly

V. Test Results

The test series began with testing the specimens in air and test durations were then duplicated for each material in the CO_2 environment. Tables 3 and 4 summarize the results for the tests in an air and CO_2 environment, respectively, and Figure 7 shows a test article during a test in air.

General observations during the test series were that most test articles experienced some gas ingestion inside of the graphite cap (evidenced by discoloration on the sides of the test samples), which may have had an effect on backface thermal response. Once the ablator recessed, a small gap opened up between the test sample and the graphite cap and allowed gas ingestion inside the cap. In addition, the thin sample size resulted in high backface temperatures at test durations required to achieve meaningful recession. The Carbon-Carbon test articles experienced the highest backface temperatures, as expected due to the high density of the material and because the test specimens did not include the insulative layer of the CC/CalCarb system. This high backface temperature caused the detachment of the RSI spacer for two of the Carbon-Carbon test specimens, thus an accurate recession measurement could not be made.

Towards the end of the test series, the slug calorimeter was experiencing anomalies that were later determined to be caused by a shorting of the thermocouple due to the vibration and constant motion of the sting arm during the entire test series. Since the facility settings and stagnation pressure data remained repeatable, the test series was completed without the slug calorimeter for test articles ARA-9018 and 3DQP test articles TB-3, TB-4, and TB-5.

Figure 8 shows recession rates in both environments for test specimens with an areal density less than 0.5 g/cm^2. Materials in this category are PICA, MonA, and PIRAS-22. The plot shows an increase in recession rate in the simulated Martian CO_2 environment for PICA and PIRAS-22. Increased recession of carbonaceous materials in CO_2 is expected due to the additional oxygen available in the dissociated CO_2 plasma stream. The additional oxidation and deeper char layer of the PICA test articles in the CO_2 environment can clearly be seen in Figure 9.

Figure 10 shows a representative PIRAS-22 pre-test specimen and post-test specimens from both an air and CO_2 test environment. Recession results for MonA were variable and Figure 8 shows one MonA test article in air with a significantly higher recession rate than the other three test articles. The manufacturing process of MonA utilizes a slurry/mixture and manufacturing processes are not yet controlled, nor optimized, due to the R&D nature of the material. Thus, material variability from specimen to specimen is the likely cause of variable recession results. Figure 11 shows a representative MonA pre-test specimen and post-test specimens tested in both environments.

Table 3. Post-test results summary for tests in air

Sample ID	Material	Cold Wall Heat Flux (W/cm^2) - Slug Calorimeter (±10%)[3]	Stagnation Pressure (kPa)	Test Time (sec)	Mass Loss (g)	Stagnation Point Recession (mm)	Peak Surface Temperature (°C)	Peak Backface Temperature (°C)
42534-1	PICA	292	3.5	15	0.40	1.346	2207	503
42534-2	PICA	293	3.5	15	0.38	1.321	2223	467
5000-1	Carbon-Carbon	273	3.5	15	0.16	N/A*	1827	777
5000-2	Carbon-Carbon	289	3.5	10	0.10	0.254	1674	606
ARA-9015	PhenCarb	297	3.5	20	1.02	0.813	2134	272
ARA-9016	PhenCarb	289	3.5	20	0.99	1.067	2137	274
BBB1	MonA	309	3.5	15	0.58	1.778	2180	341
BBB2	MonA	321	3.5	15	0.50	2.464	2121	324
BPAFG-B-01	BPAFG	297	3.5	20	0.96	2.311	2121	399
BPAFG-B-02	BPAFG	308	3.5	20	1.01	2.108	2148	391
P22-9005	PIRAS-22	298	3.5	15	0.67	0.356	2190	275
P22-9006	PIRAS-22	303	3.5	20	0.80	0.356	2192	327
Av-P42-1M	Avcoat	297	3.5	20	1.34	0.584	2080	282**
Av-P42-2M	Avcoat	304	3.5	20	1.13	0.432	2076	268
Av-P42-3M	Avcoat	306	3.5	20	1.29	0.940	2071	265
TB-1	3DQP	306	3.5	25	0.91	-0.025	1859	328
TB-2	3DQP	308	3.5	25	0.92	0.000	1852	N/A***

*RSI detachment from overheating

**no electronic cool-down data obtained

***T/C lead wire shorted to copper backplate

Table 4. Post-test results summary for tests in carbon dioxide

Sample ID	Material	Cold Wall Heat Flux (W/cm^2) - Slug Calorimeter (±10%)[3]	Stagnation Pressure (kPa)	Test Time (sec)	Mass Loss (g)	Stagnation Point Recession (mm)	Peak Surface Temperature (°C)	Peak Backface Temperature (°C)
42534-3	PICA	309	3.9	15	0.46	1.473	2218	562
42534-4	PICA	316	3.9	15	0.45	1.651	2226	560
5000-3	Carbon-Carbon	296	3.9	10	0.15	N/A*	1785	700
5000-4	Carbon-Carbon	301	3.9	10	0.15	0.254	1759	694
ARA-9017	PhenCarb	339	3.9	20	1.04	1.092	2103	273
ARA-9018	PhenCarb	Not functional	3.9	20	1.01	1.422	2080	287
BBB3	MonA	297	3.9	15	0.61	1.930	2148	339
BBB5	MonA	357	3.9	15	0.62	1.854	2141	357
BPAFG-B-03	BPAFG	346	3.9	20	1.11	2.057	2087	409
BPAFG-B-04	BPAFG	389	3.9	20	1.12	2.388	2113	422
P22-9007	PIRAS-22	300	3.9	15	0.68	0.457	2164	269
P22-9008	PIRAS-22	371	3.9	20	0.85	1.194	2174	324
Av-P43-5M	Avcoat	307	3.9	20	1.30	1.270	2109	272
Av-P43-6M	Avcoat	314	3.9	20	1.30	1.092	2109	277
TB-3	3DQP	Not functional	3.9	25	1.00	0.152	1883	N/A**
TB-4	3DQP	Not functional	3.9	25	0.96	-0.483	1880	N/A**
TB-5	3DQP	Not functional	3.9	15	0.71	0.127	1869	250

*RSI detachment from overheating

** Back of sample overheated, melted TC sheath and TC shorted to sting

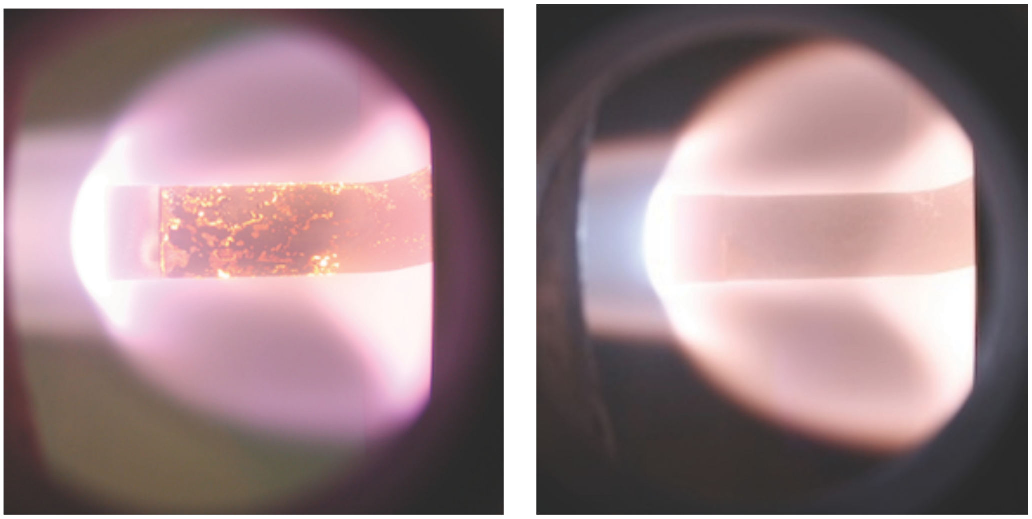

Figure 7. HYMETS test article during a test in air (left) and carbon dioxide (right)

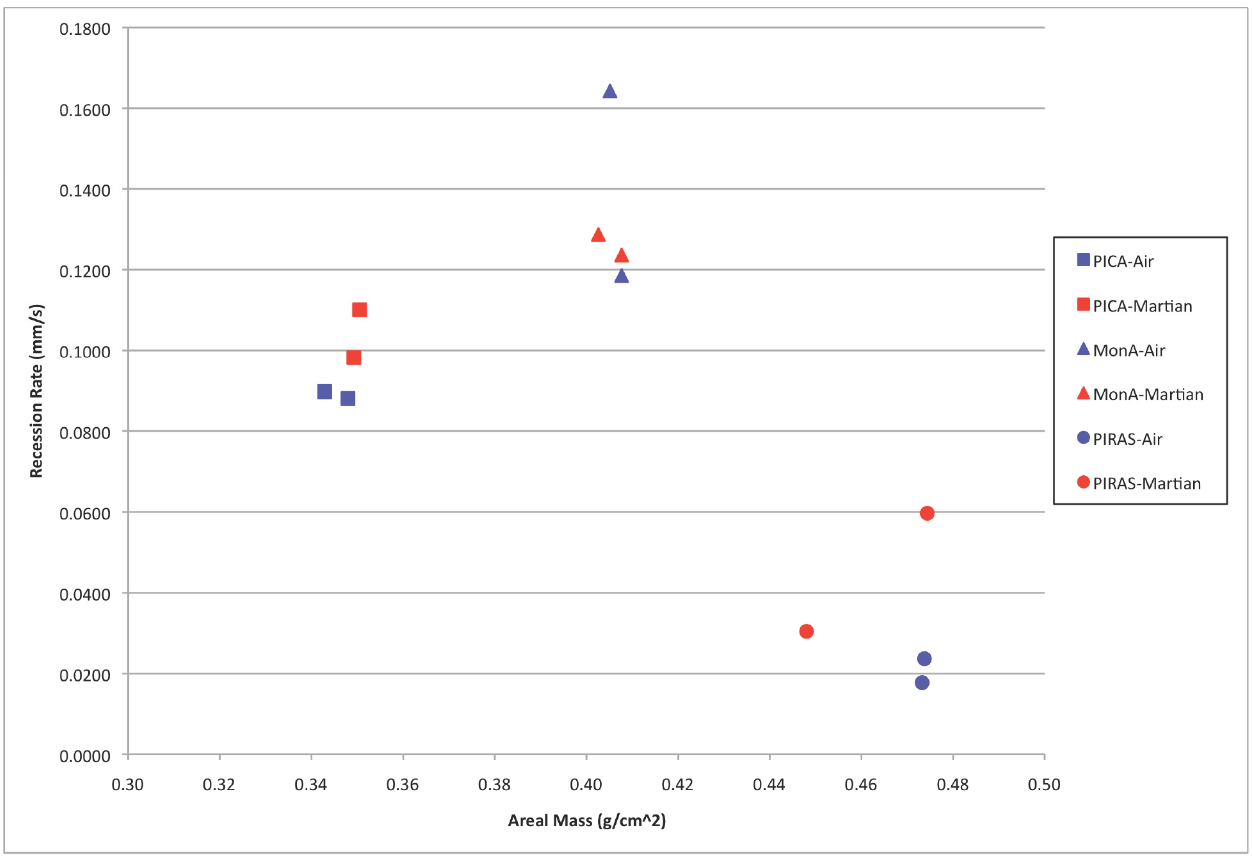

Figure 8. Recession rate by areal mass for materials with an areal mass less than 0.5 g/cm^2

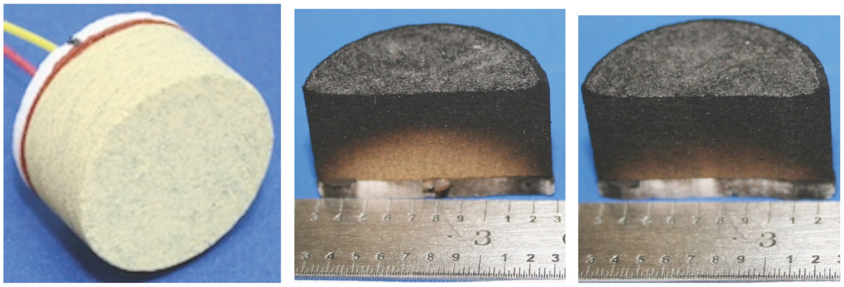

Figure 9. Pre-test photograph of PICA test article (left) and cross-section post-test images of PICA sample 42534-1 tested in air (center), and sample 42534-3 tested in carbon dioxide (right)

Figure 10. Pre-test photograph of PIRAS-22 (left); post-test photographs of test articles P22-9005 (air, center) and P22-9008 (carbon dioxide, right)

Figure 11. Pre-test photograph of MonA (left); post-test photographs of test articles BBB-1 (air, center) and BBB-5 (carbon dioxide, right)

Figure 12 shows recession rates in both environments for test specimens with an areal density greater than 0.5 g/cm^2. These materials include BPA, PhenCarb, Avcoat, 3DQP, and Carbon-Carbon. The BPA test articles showed a fairly consistent recession rate between the air and CO_2 test cases, and also experienced the highest recession rate of all the materials of approximately 0.6 g/cm^2 areal mass. Figure 13 shows pre- and post-test BPA articles. There was some variability in recession results for PhenCarb and Avcoat, but in general, there was more recession in the CO_2 environment for these two materials. Figures 14 and 15 show pre- and post-test PhenCarb and Avcoat articles, respectively. Due to the high silica content in the 3DQP test articles, these specimens experienced very little recession, and in two cases experienced expansion, due to glass melt on the surface, as seen in Figure 16. Of the two Carbon-Carbon test articles that remained intact post-test, the recession was identical for the air and CO_2 test environments. Pre- and post-test Carbon-Carbon articles are shown in Figure 17.

In conclusion, quality ablative and thermal response data, in both a simulated air and Martian environment, was obtained for all material candidates. These results, along with other thermal and structural test data, were utilized in the overall evaluation and down-selection process that will allow for further development of the most promising material candidates that will eventually satisfy the project key performance parameters.

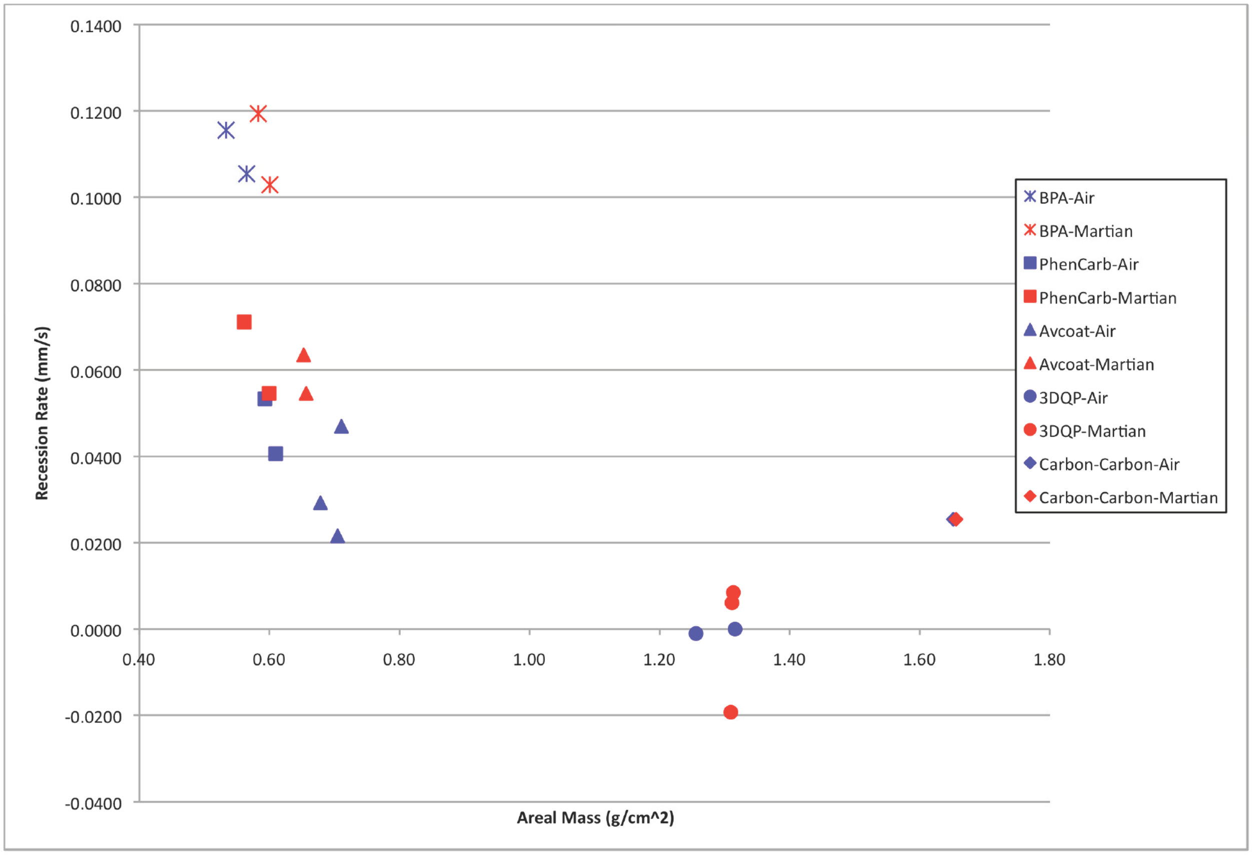

Figure 12. Recession rate by areal mass for materials with an areal mass greater than 0.5 g/cm^2

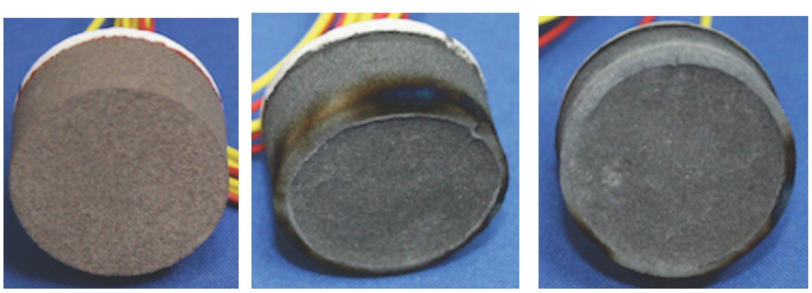

Figure 13: Pre-test photograph of BPAFG (left); post-test photographs of test articles BPAFG-B-02 (air, center) and BPAFG-B-04 (carbon dioxide, right)

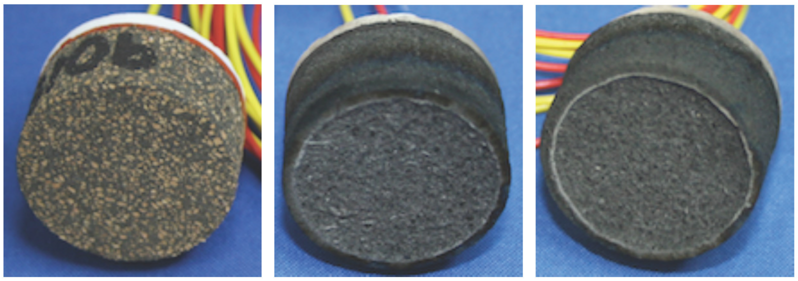

Figure 14: Pre-test photograph of PhenCarb-28 (left); post-test photographs of test articles ARA-9015 (air, center) and ARA-9018 (carbon dioxide, right)

Figure 15: Pre-test photograph of Avcoat (left); post-test photographs of test articles P42-1M (air, center) and P43-5M (carbon dioxide, right)

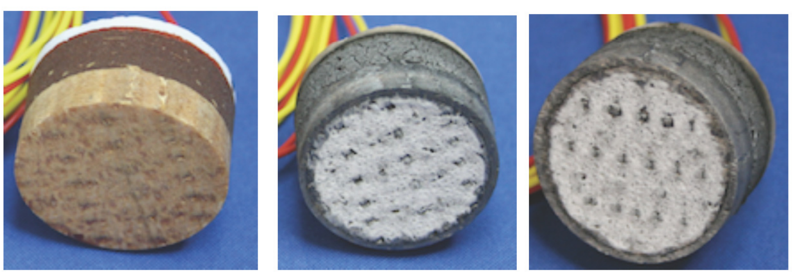

Figure 16: Pre-test photograph of 3DQP (left); post-test photographs of test articles TB-2 (air, center) and TB-4 (carbon dioxide, right)

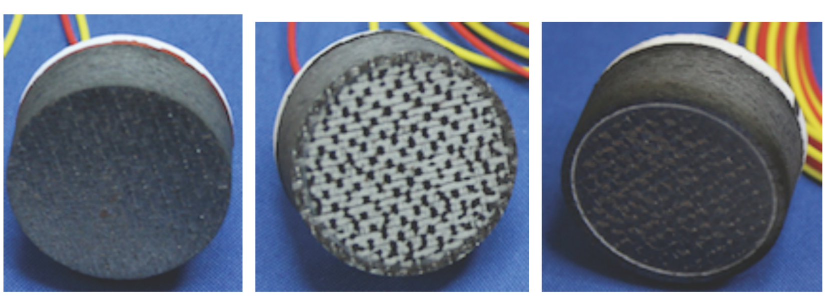

Figure 17: Pre-test photograph of Carbon-Carbon (left); post-test photographs of test articles 5000-2 (air, center) and 5000-4 (carbon dioxide, right)

VI. Summary and Conclusions

Seven rigid ablative TPS material candidates, from four different vendors, were subjected to arc jet screening tests in the HYMETS facility at NASA Langley Research Center. The test series included both a simulated air and Martian test gas environment. All test objectives were met successfully. All material candidates survived the heating condition in both environments, and some materials showed a clear increase in recession in the CO_2 environment when compared to the air environment. These test results, along with other thermal and structural test results, were utilized in the overall evaluation and down-selection process that will allow for further development of the most promising material candidates that will eventually satisfy project key performance parameters.

Acknowledgments

This test series would not have been possible without the support of numerous people at NASA Ames Research Center and NASA Langley Research Center. In particular, the authors acknowledge the efforts of Alan Cassell and Marianne Shelley for test article design and procurement, as well as Joseph Mach, Hiep Khuc, Myvan Nguyen, My Au, and Tomo Oishi for test article instrumentation and final assembly. The authors also acknowledge Bernie Laub for his expert guidance in the evaluation of ablative materials. This test series was performed under the leadership of Robin Beck, Michael Wright, Helen Hwang, and Paul Krasa. The work of the first author was carried out at the Jet Propulsion Laboratory, California Institute of Technology, under a contract with the National Aeronautics and Space Administration.

References

[1]Cassell, A., Beck, R., Arnold, J., Hwang, H., Wright, M., Szalai, C., Blosser, M., Poteet, C., "Development of Thermal Protection Materials for Future Mars Entry, Descent, and Landing Systems," AIAA 2010-5049, 10th AIAA/ASME Joint Thermophysics and Heat Transfer Conference, Chicago, Illinois, 28 June – 1 July 2010.

[2]Splinter, S., Bey, K., Gragg, J., Brewer, A., "Comparative Measurements of Earth and Martian Entry Environments in the NASA Langley HYMETS Facility," AIAA-2011-1014, 49th Aerospace Sciences Meetings, Orlando, Florida, 4 January – 7 January 2011.

[3]Nawaz, A., Santos, J.A., Assessing Calorimeter Evaluation Methods in Convective and Radiative Heat Flux Environment, AIAA 2010-4905, 10th AIAA/ASME Joint Thermophysics and Heat Transfer Conference, Chicago, Illinois, 28 June – 1 July 2010.